Giant and Tunable Goos–Hanchen Shifts for Attenuated Total Reflection Structure Containing Graphene

Gadum Pertin

Peace Panmei

Debashish Sonowal

Electronics and Instrumentation Engineering
National Institute of Technology
Agartala-799055, INDIA
April-2022

Giant and Tunable Goos–Hanchen Shifts for Attenuated Total Reflection Structure Containing Graphene

Report submitted to

National Institute of Technology, Agartala

for the award of the degree

of

Bachelor of Technology

by

Gadum Pertin (18UEI018)

Peace Panmei (18UEI022)

Debashish Sonowal (18UEI038)

Supervisor:

Dr. Aparupa Kar

ELECTRONICS AND INSTRUMENTATION ENGINEERING

NATIONAL INSTITUTE OF TECHNOLOGY, AGARTALA

APRIL-2022

APPROVAL SHEET

This report entitled (Giant and Tunable Goos–Hanchen Shifts for Attenuated Total Reflection Structure Containing Graphene) by (Aparupa Kar) is approved for the degree of _____ (Degree details).

Examiners

_____
_____
_____

Supervisor (s)

_____
_____
_____

Chairman

_____

Date: _____

Place: _____

DECLARATION

I declare that this written submission represents my ideas in my own words and where others' ideas or words have been included, I have adequately cited and referenced the original sources. I also declare that I have adhered to all principles of academic honesty and integrity and have not misrepresented or fabricated or falsified any idea/data/fact/source in my submission. I understand that any violation of the above will be cause for disciplinary action by the Institute and can also evoke penal action from the sources which have thus not been properly cited or from whom proper permission has not been taken when needed.

_____

(Signature)

Gadum Pertin
Peace Panmei
Debashish Sonowal
(Name of the students)

18UEI018
18UEI022
18UEI038
(Roll No.)

Date:

CERTIFICATE

It is certified that the work contained in the thesis titled “Giant and Tunable Goos–Hanchen Shifts for Attenuated Total Reflection Structure Containing Graphene” by “Gadum Pertin, Peace Panmei, Debashish Sonowal” has been carried out under my/our supervision and that this work has not been submitted elsewhere for a degree*

Signature of Supervisor
Aparupa Kar
Electronics and Instrumentation Engineering
N.I.T. Agartala
April, 2022

ACKNOWLEDGEMENT

We wish to express our sincere gratitude to Dr. Aparupa kar, our project guide, Electronics & Instrumentation Department of National Institute of Technology, Agartala for providing us an opportunity to do our project work on “Giant and Tunable Goos–Hanchen Shifts for Attenuated Total Reflection Structure Containing Graphene”. She guided and explained to us every topic in detail. With the knowledge she imparts through her remarkable explanation and guidance, we were able to be finished this project within the stipulated time. We would also like to underscore the dynamic efforts of the teamwork and the effort given by the whole team. This project bears the imprint of many people. I sincerely thank my project guide for guidance and encouragement in carrying out this project work. Last but not least we wish to avail ourselves of this opportunity to express a sense of gratitude and love to our friends and our beloved parents for their manual support, strength, and for everything.

Contents

ABSTRACT

The Goos–Hänchen (GH) shift is one of the important aspects to evaluate the performance of multilayer surface plasmon resonance (SPR) sensors. In this paper, in order to design the optimal SGH (Spatial Goos Hanchen Shift) and AGH (Angular Goos Hanchen) shifts we have worked on how we change and manipulate the chemical potential that will be affecting these shifts. We have used the otto and Kretschmann configurations to observe the shifts. The comparison of these graphs about the shifts have been compared. It is being observed like how a slight change in the wavelengths is affecting the shifts. We have mention the characteristics of graphene its conductivity, etc. In the beginning of the project we have observe about the surface plasmon and surface plasmon resonace over a metallic surfaces that affecting the electromagnetic wave. The electromagnetic wave that have been focused is the P-Polarized EM wave that how it's beam being reflected over the Otto and Kretschmann configuration. Finally, we have concluded over the relationships by modulating the voltage applied to graphene via an external gate, the GH shifts can be controlled. The superior sensitivity of the SP sensor can be obtained by using an alternative SP sensing scheme based on the giant and tunable GH shift.

CHAPTER - 1: INTRODUCTION

A spatially limited optical beam on reflection/transmission or total internal reflection at an optical interface, violate the geometric optics prediction thereby indicating diffractive corrections such as Goos–Hänchen (GH) shift. GH shift is the longitudinal displacement occurring in the plane of incidence relative to the geometric optics position for an incident linearly polarized beam. The wide area of applications of the GH shift has made these shifts technically significant in recent years. The GH shift is polarization-dependent and manifests a spatial character elucidating the displacement of the beam with respect to the geometrical ray and an angular character depicting the angular deviation of the beam from the law of specular reflection. The extremely small magnitudes of this shift as compared to the finite transversal extent of the incident beam have limited their applications mostly to laboratories. A great deal of literature exists about the endeavor to enhance this shift by exploring new optical structures with various materials and configurations at a wavelength other than the telecommunication wavelength within C-band (1550 nm). The magnitude of this shift can also be magnified by utilizing the long-range surface Plasmon polarization (LRSPP) resonance phenomenon. Surface plasmon polarizations (SPPs) are transverse magnetic (TM) polarized optical surface waves that propagate along with a metal-dielectric interface. LRSPP is formed by the coupling of two SPPs at the opposite boundary of a metal film sandwiched between two semi-infinite dielectric media. Further, it is highly desirable for a variety of optical device applications, to realize the tunability of lateral shift in a fixed configuration or device based on thermal-optic, electro-optic, acousto-optic, and all-optic effects. Various techniques have been proposed for tuning optical beam shifts.

When a polarized monochromatic Gaussian beam strikes the base of a dielectric prism having a higher refractive index, at an angle greater than the critical angle, a total internal reflection of the light beam occurs from the bottom of the prism with an appearance of the evanescent wave which penetrates a distance about a wavelength under the prism. When for a certain angle of incidence, the inplane wavenumber of incident light matches the propagation constant of the surface plasmon mode, surface plasmon resonance takes place. This method is called the “attenuated-total-reflection” method as around the surface plasmon resonant angle, coupling of high concentration of energy from the incident beam into the surface plasmon

mode occurs, which is accompanied by strong suppression of the reflected light intensity. Due to the longer propagation length of the surface plasmon mode and extended penetration depth of the evanescent field into the dielectric medium in the case of surface plasmon mode, the GH shift gets enhanced at the surface plasmon resonant angle.

CHAPTER - 2: Surface Plasmon Resonance

The existence of this surface plasmon phenomenon was extensively studied by many scientists. The first observation of this surface plasmon was reported by Wood in the year 1902, whereas the theoretical investigation of this phenomenon was carried out by Zenneck. The versatility of this technique was explored by Otto, Kretschmann, Raether, Agarwal, Swalen. In the term “surface plasmon”, the word “plasmon” comes from the term “plasma” and a brief description towards this “plasma” is depicted in the following section.

2.1 PLASMA

In the universe, there are four different states of matter: solid, liquid, gas and plasma. Plasma can be thought of as two gases intermixed – a gas of electrons and a gas of ions. On account of the average strength of the electrical forces in the plasma, it is neutral. At very low temperature, matter exists in solid state where the atoms are arranged in well-organized grid. On increasing the temperature above a critical value, solid melts and becomes liquid where the grid of atoms is broken, but molecular bonds are maintained. When the liquid is heated above a second critical temperature, it turns into gas. Now further heating this gas will ionize its molecules or atoms (reduce or increase the number of electrons in them), thus turning it into plasma, which contains charged particles: positive ions and negative electrons. The somewhat independent movement of the positive and negative charges makes the plasma electrically conductive, due to which it responds strongly to electromagnetic fields. Like gas, plasma does not have a definite shape or a definite volume. In the influence of a magnetic field, it may form structures such as filaments, beams and double layers. Plasma was first identified in a Crookes tube and so described by Sir William Crookes in the year 1879 (He called it radiant matter). The nature of this was identified by British physicist Sir J.J. Thomson in the year 1897.

2.2 PLASMONS

Plasmons are defined as coupled electromagnetic or electronic wave that appears inside and on the surface of metals and other materials, and have the ability to confine light to nanoscale regions. Plasmon can also be identified by the quantized oscillation of electrons in the metal's conduction band or by the quantum of plasma oscillation. This plasma oscillation or waves of plasma are an interconnected set of particles and fields which propagates in a periodically repeating fashion and composed of electrons and a single species of positive ions, but it may also contain multiple ion species including negative ions as well as neutral particles.

The plasma oscillation can be classified by the oscillating species. In most plasmas of interest, the electron temperature is comparable to or larger than the ion temperature. This fact, coupled with the much smaller mass of the electron, implies that the electrons are much faster than the ions. An electron mode depends on the mass of the electrons and an ion mode depends on the ion mass where the ions may be assumed to be infinity massive that is stationary and the electrons are assumed to be mass less and to redistribute themselves instantaneous according to the Boltzmann relation. Thus, plasmons are collective oscillations of the free electron gas density, often at optical frequencies. They can also couple with a photon to create a third quasiparticle called a plasma polariton.

2.3 SURFACE PLASMON

Now surface plasmons are those plasmons that are confined to metals surfaces and interact strongly with light resulting in a polariton or longitudinal charge density oscillations. Or we can say surface plasmons (SPs) are coherent electrons oscillations existing at the interface between two materials where the real part of the dielectric function changes sign across the interface (e.g. a metal-dielectric interface, such as a metal sheet in air). The coupling of SPs with photons results in the hybridized excitation called surface plasmon polariton (SPP). The propagation length of this SPP along the metal surface is decided by energy lost either via absorption in the metal or radiation into free space. This phenomenon was first observed by "Wood" in the year 1902 and its existence was first predicted by R. H. Ritchie in the year

1957. In the following two decades, surface plasmons were extensively studied by many scientists, the foremost of whom were Heinz Raether, E. Kretschmann and A. Otto.

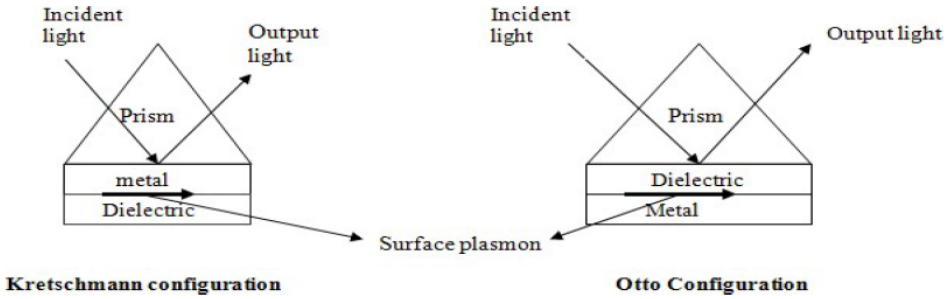

Fig. Kretschmann and Otto configuration for excitation of Surface Plasmons

Surface plasmon resonance (SPR) is one of the most promising optical techniques that find application in different fields. The first sensing application through the SPR technique was reported in 1983 and since then numerous SPR sensing structures for chemical and biochemical sensing have been reported. In the SPR technique, a p-polarized light causes the excitation of surface plasmons (SPs) at the metal-dielectric interface. When the energy as well as the momentum of the incident light and SPs match, a resonance appears which results in a sharp dip in the reflected light intensity. In the surface plasmon resonance (SPR) phenomenon, energy and momentum are transferred from incident photons into the plasmons for specific resonance conditions of -

1) Incident light (p-polarized),
2) Angle of incidence,
3) Wavelength,
4) Refractive indices of the dielectric and metal,
5) Metal and dielectric layer thicknesses.

The surface plasmons are accompanied by a longitudinal electric field that decays exponentially in metal as well as in dielectric medium. The electric field is maximum at the metal-dielectric interface. The exponential decay of the electric field is found by solving Maxwell's equation for semi-infinite media of metal and dielectric with an interface of metal-dielectric. The propagation constant (Ksp) of the surface plasmon wave propagation along with the metal-dielectric interface

is given by

$$-K_{sp} = \frac{\omega}{c}\sqrt{\frac{\varepsilon_m \varepsilon_i}{\varepsilon_m + \varepsilon_i}}$$

are ε_m and ε_i are the dielectric constants of metal and dielectric medium respectively, ω is the angular frequency of the incident light and c is the velocity of light in vacuum.

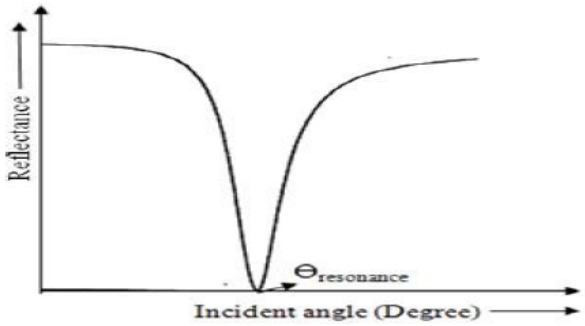

Reflectivity vs. incident angle graph of Surface Plasmon Resonance

When a light beam is an incident on the base of the prism (as an optical component) at an angle greater than the critical angle then a total internal reflection of the light beam takes place at the prism air interface. As in total internal reflection, the light beam returns after penetrating in the lower refractive index medium. The field in the lower refractive index medium is called evanescent field and the wave corresponding to this is called evanescent wave. The evanescent wave propagates along with the prism-air interface and decays exponentially in the rarer medium. The propagation constant of the evanescent wave, at the prism-air interface is expressed as

$$k_{ep} = \frac{\omega}{c}\sqrt{\varepsilon_p}\sin\theta$$

Where ε_p represents the dielectric constant of the optical material and θ is the angle of incidence of the incident beam. Thus the resonant angle, θ_{res} for surface plasmon resonance condition can be found through the following equation –

$$\frac{\omega}{c}\sqrt{\varepsilon_p}\sin\theta_{res} = \frac{\omega}{c}\sqrt{\frac{\varepsilon_m\varepsilon_i}{\varepsilon_m+\varepsilon_i}}$$

The resonant angle is very sensitive to variation in the refractive index of the sensing layer. From the reflectance vs. incident angle graph of SPR, it is clear that at resonant angle reflectance is zero or minimum and it increases with the increase in incident angle.

CHAPTER - 3: TOTAL INTERNAL REFLECTION

Total internal reflection (TIR) is the optical phenomenon in which waves arriving at the interface (boundary) from one medium to another (e.g., from water to air) are not refracted into the second ("external") medium, but completely reflected back into the first ("internal") medium. It occurs when the second medium has a higher wave speed (lower refractive index) than the first, and the waves are incident at a sufficiently oblique angle on the interface. For example, the water-to-air surface in a typical fish tank, when viewed obliquely from below, reflects the underwater scene like a mirror with no loss of brightness.

3.1 TOTAL INTERNAL REFLECTION INDUCED OPTICAL BEAM SHIFTS

In the arena of light-matter interaction, Total Internal Reflection (TIR) is the phenomenon where the complete reflection of a propagated wave into the incident medium is found, when it strikes a less dense medium boundary at an angle greater than the critical angle. The critical angle is the angle of incidence where the refracted ray lies along the boundary, having an angle of refraction of 90°. When a light beam of finite transversal extent undergoes TIR from an interface between two different dielectric media, its behavior displays a deviation from that exhibited by the plane waves which can be identified by the diffractive corrections such as Goos-Hänchen (GH) shift and the Imbert-Fedorov (IF) shift.

3.2 GH SHIFT

The Goos–Hänchen shift refers to the lateral displacement occurring in the plane of incidence, that a wave having finite cross section undergoes when it is total internally reflected at an interface of two media having different indices of refraction due to the propagation of an evanescent wave parallel to the interface. Theories of this lateral shift in total internal reflection of electromagnetic waves were developed by Schaefer and Pich whereas the first measurement of this lateral displacement was done by Goos and Hänchen. Their experimental works expedite the way of new theoretical works by Artmann and V. Fragstein , where expressions for the lateral shift were obtained for incident light polarization parallel to or perpendicular to the plane of incidence. Wolter carried out a measurement of the Goos-Hänchen shift that was in good agreement with theory.

Later in the year 1970, an historical overview of both theory and experiment related to the GH shift was given by H. K. V. Lotsch. Puri and Birman also provided a survey of early work on the GH shift as well as more recent extensions involving spatially dispersive media and the role played by surface plasmon polaritions.

Assuming that the magnetic permeability constant of each medium is approximately equal to unity, the GH shift for the incident light electric field polarization perpendicular to the plane of incidence, is

$$D_{\perp} = -\frac{1}{k}\frac{d(\phi)_{\perp}}{d\theta} = \frac{\lambda}{\pi}\frac{\sin\theta}{\sqrt{\sin^2\theta - n^2}}$$

For electric field polarization parallel to the plane of incidence, the GH shift is

$$D_{\parallel} = -\frac{1}{k}\frac{d(\phi)_{\parallel}}{d\theta} = \frac{n^2}{\sin^2\theta(1+n^2) - n^2} D_{\perp}$$

where $k = \frac{2\pi}{\lambda}$, θ represents the incident angle, ϕ represents the reflection phase and λ represents the incident light wavelength.

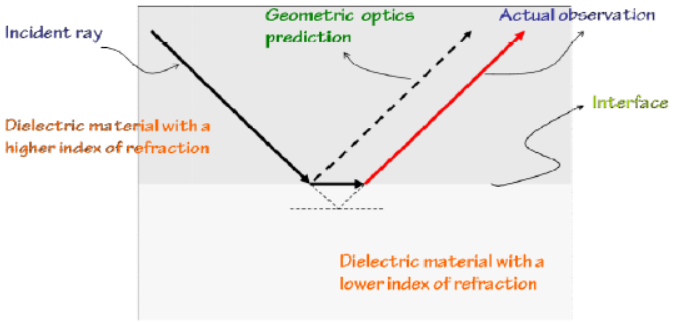

Fig. Goos–Hänchen (GH) shift in total internal reflection of light in a glass-air system.

These equations were derived by Artmann and valid only near the critical angle. Artmann explained the effect by expanding the incident beam into its plane wave components, each with a slight different transverse wave vector. Then, each plane wave component undergoes a slight different phase change after total internal reflection so that the sum of all the reflected plane waves, which forms the reflected beam, results in a lateral shift of the intensity peak, which is given by

$$S = -\frac{1}{k}\frac{d\phi}{d\theta}$$

where k is the wave vector in the medium of incidence, θ is the incident angle, and ϕ is the phase difference between the reflected and incident waves.

CHAPTER - 4: GRAPHENE

Graphene is a one-atom-thick tightly packed layer of carbon atoms bonded together in a hexagonal honeycomb lattice. It is an allotrope of carbon in the structure of a plane of sp2 bonded atoms with a molecule bond length of 0.142 nm. Carbon has many different forms, from the graphite found in pencils to the world's most expensive diamonds. In 1980, only three basic forms of carbon were known, namely diamond, graphite, and amorphous carbon. After that, fullerenes and carbon nanotubes were discovered and, in 2004, graphene joined the club. It is the building-block of Graphite where layers of graphene are stacked on top of each other with an interplanar spacing of 0.335 nm.

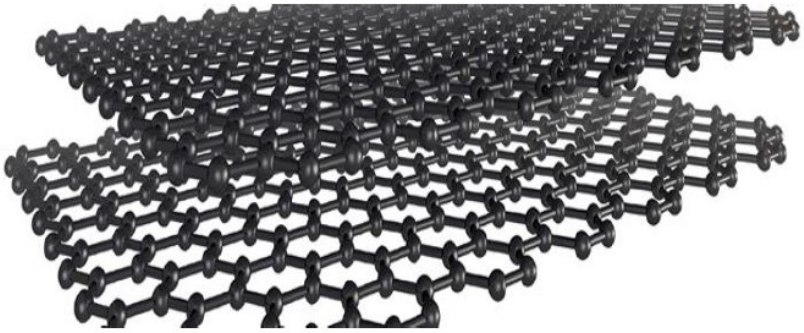

Fig. Graphene

It is the strongest compound discovered (between 100-300 times stronger than steel and with a tensile stiffness of 150,000,000 psi), the lightest material known (with 1m2 coming in at around 0.77 milligrams), the best conductor of heat at room temperature (at (4.84±0.44)×103 to (5.30±0.48)×103 W·m−1·K−1) and also the best conductor of electricity known with electron mobility at values of more than 15,000 cm2·V−1·s−1). It also has unique levels of light absorption at πα ≈ 2.3% of white light, and possesses potential suitability for use in spin transport. These astonishing properties have earned it the title “wonder material”.

The discovery of graphene, made by a physics professor and his PhD student in a laboratory in Manchester, using a piece of graphite and some Scotch tape has completely revolutionized the way we look at potential limits of our abilities as scientists, engineers and inventors. Since its discovery, it has undoubtedly emerged as one of the most promising nanomaterials

having advancements within different scientific disciplines with huge gains being made particularly in electronics and biotechnology already.

4.1 GRAPHENE POTENTIAL APPLICATIONS

Graphene manifests great potential applications in nanoelectronic devices and optoelectronic devices with ultrahigh electron mobility, ultrafast relaxation time for photo-excited carriers, and gate-variable optical conductivity on account of its exceptional electrical, mechanical, thermal, and optical properties, which comprise strong light-graphene interaction, broadband and high-speed operation, etc. The potential applications in optoelectronic devices include graphene touch screens with the advantage of improving performance and reducing costs, the grapheme based optical modulator having the benefit of ultrafast modulation speed across a broad range of wavelengths, graphene photodetectors having high responsivity and ultra-broadband at room temperature, the epitaxial graphene transistors with high frequency performance, the gate voltage tunable and controllable graphene's plasmons leading to an advantage over surface plasmons at metal-dielectric interface, and the graphene based broadband polarizer having an extinction ratio approximately upto 27 dB in the telecommunications band, etc. Apart from the linear response of the graphene, it also exhibits admirable nonlinear characteristics. Hendry et al. discovered that the graphene's third-order optical susceptibility is only weakly dependent on the wavelength in the near-infrared frequency range. Gullans et al. showed that in graphene nanostructures it was probable to realize noteworthy nonlinear optical interactions at the few photon levels. Sun et al. and Bao et al. exploited the optoelectronic properties of grapheme for the realization of ultrafast lasers and saturable absorbers. Wang et al.reported a broad optical limiting (at 532 and 1,064 nm) through liquid-phase exfoliation for nanosecond pulses. Zhang et al. reported that graphene has a giant nonlinear refractive index $n2 \simeq 10{-}7$ cm2 W−1, almost 9 orders of magnitude larger than bulk dielectrics.

Therefore more fortunately, it is shown that graphene possess the large nonlinear Kerr index and ultrafast nonlinear response at the broad band of frequencies, which in turn offers the probability of realizing the optical bistable devices under actual experimental conditions. Hence owing to its superior third-order nonlinear optical properties, recently graphene photonics have been stretched to nonlinear optical bistable devices. Through deposition of

graphene with silicon photonic crystal cavity, Gu et al. achieved ultralow-power resonant optical bistability, coherent four-wave mixing and self-induced regenerative oscillations. Theoretical investigation of the optical bistability of reflection at the interface between graphene and Kerr-type nonlinear substrates was performed by Xiang et al. Horvath et al. reported optical bistability in a graphene–silicon waveguide resonator. Peres et al. found optical bistability in the lower THz frequency range for a single layer of nonlinear graphene in aerial suspension. Recently, Bao et al. demonstrated graphene nanobubbles to be a promising type of optical nonlinear medium which can circumvent the limitation of optical path length in atomically thin two-dimensional films, and so that all optical switching and optical bistability are obtained in this graphene nanobubbles.

4.2 Optical Response of Graphene sheets

The optical response of graphene sheet is characterized by its surface conductivity (б). Therefore ignoring the impact of magnetic field (without Hall conductivity) and under Kubo formation, the complex optical-linear conductivity of graphene, $б_0$ is expressed as the contribution of intraband, $б_{intra}$ and interband, $б_{inter}$ terms

$$\sigma_{intra} = \frac{ie^2 2k_B T}{\pi\hbar^2(\omega + i\tau^{-1})}\left\{\frac{E_F}{2k_B T} + \ln\left[1 + \exp\left(-\frac{E_F}{k_B T}\right)\right]\right\}$$

$$\sigma_{inter} = \frac{e^2}{4\hbar}\left(\frac{1}{2} + \frac{1}{\pi}\tan^{-1}\left(\frac{\hbar\omega - 2E_F}{2k_B T}\right) - \frac{i}{2\pi}\ln\left|\frac{(\hbar(\omega + i\tau^{-1}) + 2E_F)^2}{(\hbar(\omega + i\tau^{-1}) - 2E_F)^2 + 4(k_B T)^2}\right|\right)$$

The dependence of Fermi energy (E_F) on the carrier density for a graphene sheet (η_{2D}) is given by-

$$E_F = \hbar v_F \sqrt{\pi \eta_{2D}}$$

and

$$\eta_{2D} = \frac{C_g}{e}(V_g - V_{dirac})$$

Where C_g , V_g, V_{dirac}, e represent the gate capacitance, gate voltage, gate voltage corresponding to the charge neutral Dirac point and electron charge respectively.

Therefore, n_{2D} is electrically controlled by the gate voltage application on graphene which leads to a relation of voltage controlled Fermi energy for graphene sheet. T represents the temperature in K, ω denotes the angular frequency of incident light, τ is the electron-phonon relaxation time, v_F signifies the Fermi velocity of electrons (=106 m/s), e , k_B and $\hbar$ are related to electron charge, Boltzmann constant and reduced Plancks constant respectively.

Owing to the electrical tunability of its surface conductivity by modulating its charge carrier density through electrostatic doping using an external gate voltage, graphene has been recognized as a promising candidate for the designing of tunable optical sensors, tunable meta-materials and tunable terahertz absorbers etc. that operates in both THz and optical frequency ranges. As a consequence of tunable optical conductivity, the graphene SPP spectrum can be dynamically tuned through electrical and chemical doping.

CHAPTER - 5: BOUNDARY CONDITIONS OF EM WAVE FOR THE P- POLARIZED WAVES

In the former ATR structures, plasmonic materials are noble metal or left-handed meta-material, which is hardly tuneable and exhibits large losses. More recently, it has been found that SP modes can also be supported in graphene, a single layer of carbon atoms gathered in a honeycomb lattice, at infrared and terahertz frequencies. By applying a gate voltage, the transport properties of graphene can be readily modulated and can be applied to various plasmonic devices.

A linear-polarized electromagnetic (EM) wave with frequency ω impinges on the interface between region 1 (with a dielectric constant ε1) and region 2 (with a dielectric constant ε2) and a graphene layer sandwiched between region 2 and region 3 (with a dielectric constant ε3). It is assumed that the incident wave is a monochromatic beam of wavelength λ0 and waist w0; the media in three regions are all nonmagnetic, and all these dielectric constants are real. Since the system is uniform in the x direction, we can decompose the EM field En, Hn and n = 1, 2, 3; into two components and consider the s (TE) - and p (TM)-polarized waves separately. For simplicity, we only discuss the p-polarized case in the following plane of incidence (yz), and we have for the p-polarized waves, the magnetic field vector is perpendicular to the plane of incidence (yz), and we have Hn = {Hnx, 0, 0} and En = {0, Eny, Enz}. The magnetic fields of the p-polarized waves for three regions are:

$$\begin{cases} H_1 = Ae^{ik_{1z}(z+d)+ik_y y} + R \cdot e^{-ik_{1z}(z+d)+ik_y y}, \\ H_2 = Be^{ik_{2z}z+ik_y y} + Ce^{-ik_{2z}z+ik_y y}, \\ H_3 = T \cdot e^{ik_{3z}z+ik_y y}, \end{cases}$$

$$\text{where } k_{nz} = \sqrt{k_n^2 - k_y^2},\ k_n = \omega\sqrt{\varepsilon_n}/c = k_0\sqrt{\varepsilon_n} = \omega\sqrt{\varepsilon_0\varepsilon_n\mu_0},$$

A, B, and C are constants with respect to position, and R and T denote the reflection and transmission coefficients respectively. If the angle of incidence θi is larger than the critical

angle of total internal reflection $\theta c = \arcsin[\max(\varepsilon 2, \varepsilon 3)/\varepsilon 1]$. The EM wave in region 2 will be evanescent in the z direction and $k_{2z} = i\kappa_{2z} = i\sqrt{(ky^2 - k2^2)}$. The same is true for the field in region 3, $k3z = i\kappa 3z = i\sqrt{(k^2{}_y - k^2{}_3)}$.

\

CHAPTER - 6: THE EXPRESSION OF SGH AND AGH SHIFT

According to Maxwell equations $\nabla \times Hn = -i\omega\varepsilon_0\varepsilon_n En$, the expression of electric fields for three regions can be derived. At the interface $z = -d$, the continuity of tangential components of the electric and magnetic fields yields. So, the boundary conditions will become at the interface $z = -d$, $E_{1x,\,1y}(y, -d) = E_{2x,\,2y}(y, -d)$, $H_{1x,\,1y}(y, -d) = H_{2x,\,2y}(y,-d)$, at the interface $z = 0$, $E_{3x,\,3y}(y,0) = E_{2X,2Y}(y,0)$. Hence from the above two conditions we obtain that: $H_{3x}(y, 0) - H_{2x}(y, 0) = -\sigma(\omega)E_y(y,0)$, $H_{3y}(y, 0) - H_{2y}(y, 0) = \sigma(\omega)E_x(y, 0)$.

Matching those boundary conditions, we can obtain expressions for R and T as

$$R = R_m e^{i\varphi_R}\ ,\quad T = T_m e^{i\varphi_T}\ ;$$

where φ_R and φ_T are the phases of the reflection and transmission coefficients, R_m and T_m representing the amplitude of the reflection and transmission coefficients respectively.

Hence, we finally obtain the equations for SGH shift and AGH shift as :

SGH shift = $\Delta_{R,T} = -(1/k_1 \cos\theta_i)\partial\varphi_{R,T}/\partial\theta_i$

AGH shift = $\Theta_R = -(\theta_0^2/2R_m)\partial R_m/\partial\theta_i$

where $\theta_0 = 2\lambda_0/\omega_0$ is the angular spread of the incident beam.

CHAPTER - 7: GRAPHENE AND THE CHEMICAL POTENTIAL

Each graphene monolayer can be considered as a surface conducting sheet. Near the THz regime, intraband scattering dominates in highly doped graphene, and its conductivity appears in a Drude-like form $\sigma \approx ie^2\mu/[\pi\hbar^2(\omega+i\tau^{-1})]$, where μ is the chemical potential and τ is a phenomenological electron relaxation time. The value of chemical potential depends on the carrier density and can be controlled by gate voltage. For all following calculations, τ is taken to be 1 ps. Assuming that the frequency of the impinging radiation lies in the spectral region where $Im(\sigma) > 0$, p-polarized SPs can be induced in graphene. When the tangential component of the wave vector of the incident beam coincides with the wavenumber of the SP, the interface between the second and third region, supports SPs that can be excited resonantly, resulting in a drastic decrease of the reflectivity. The SP dispersion may be derived as $\varepsilon 3 k3z + \varepsilon 2 k2z + \sigma\omega\varepsilon_0 = 0$, from which the propagation constant of SP can be derived as $ksp \approx \pi\varepsilon 0\hbar 2\ (\varepsilon_3 + \varepsilon_2)(\omega^2 + i\omega\tau^{-1})e^2\mu$.

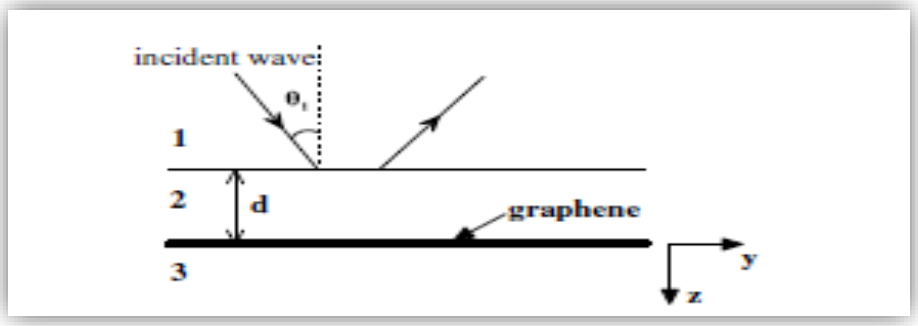

Fig. ATR structure (Otto configuration) containing a graphene layer

The value of chemical potential depends on the carrier density and can be controlled by gate voltage. When the tangential component of the wave vector of the incident beam coincides with the wavenumber of the SP, the interface between the second and third region in as shown in the fig. shows that it supports SPs that can be excited resonantly, resulting in a drastic decrease of the reflectivity.

CHAPTER - 8: IMPLEMENTATIONS WITH CHEMICAL POTENTIAL USING MATLAB

The SP dispersion may be derived as $\varepsilon_3 k_{3z} + \varepsilon_2 k_{2z} + \sigma\omega\varepsilon_0 = 0$, from which the propagation constant of SP can be derived as $k_{sp} \approx \pi\varepsilon_0\hbar^2(\varepsilon 3 + \varepsilon 2)(\omega^2 + i\omega\tau^{-1})/e^2\mu$. The absolute value of the reflection coefficient has a deep minimum, and giant lateral beam shifts are expected at the angles of incidence such that the beam spectrum contains the components with the same k_y as the wavenumber of the SP.

We can obtain explicit expressions for R ($R = R_m e^{i\varphi_R}$) and T ($T = T_m e^{i\varphi_T}$) where φ_R and φ_T are the phases of the reflection and transmission coefficients, R_m and T_m represent the amplitude of the reflection and transmission coefficients respectively. The form of the SGH shifts can be given by

SGH shift = $\Delta_{R,T} = -(1/k_1 \cos\theta_i)\, \partial\varphi_{R,T}/\partial\theta_i$

And the AGH shifts can be expressed as

AGH shift = $\Theta_R = -(\theta^2_0/2R_m)\, \partial R_m/\partial\theta_i$

When the tangential component of the wave vector of the incident beam coincides with the wavenumber of the SP, the interface between the second and third region supports SPs that can be excited resonantly, resulting in a drastic decrease in the reflectivity.

8.1 REFLECTIVITY OF EM WAVES WITH DIFFERENT CHEMICAL POTENTIALS

We can obtain explicit expressions for R ($R = R_m e^{i\varphi_R}$) and T ($T = T_m e^{i\varphi_T}$) where φ_R and φ_T are the phases of the reflection and transmission coefficients, R_m and T_m represent the amplitude of the reflection and transmission coefficients respectively.

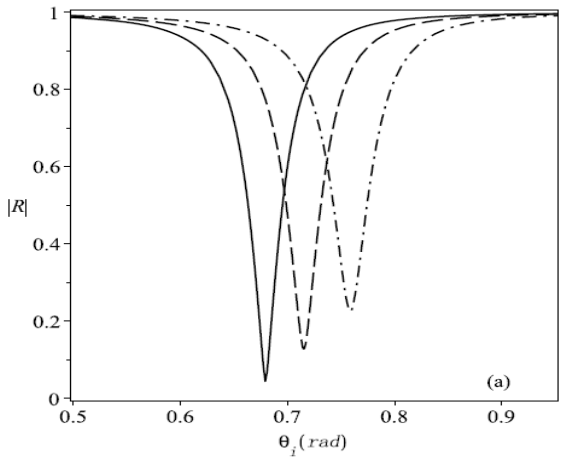

Fig. Reflectivity of EM waves with different chemical potential μ versus incident angle. Solid line indicates μ=1.4 eV, dashed line μ= 1. 3 eV, and dashed-dotted line μ =1.2 eV. Other parameters are ε_1 =16, ε_3= 2.5, ε_2 = 1.0, d= 3 μm, and ω =5 THz.

As we know that the gate voltage application on graphene which leads to a relation of voltage controlled Fermi energy for graphene sheet. As a consequence of tunable optical conductivity, the graphene SPP spectrum can be dynamically tuned through electrical and chemical doping.

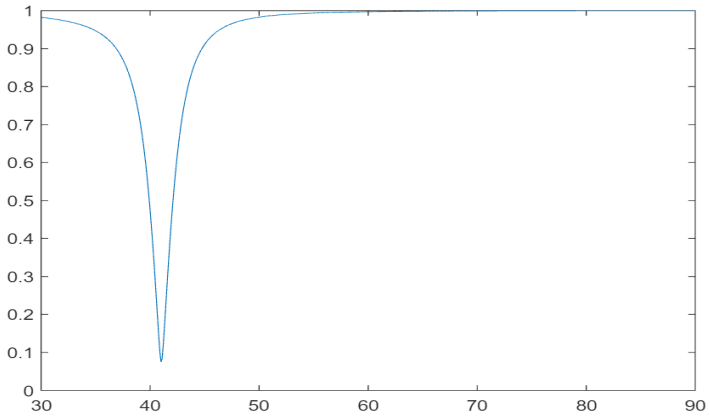

Fig. 8.1 a. From the graph where μ=1.2 eV

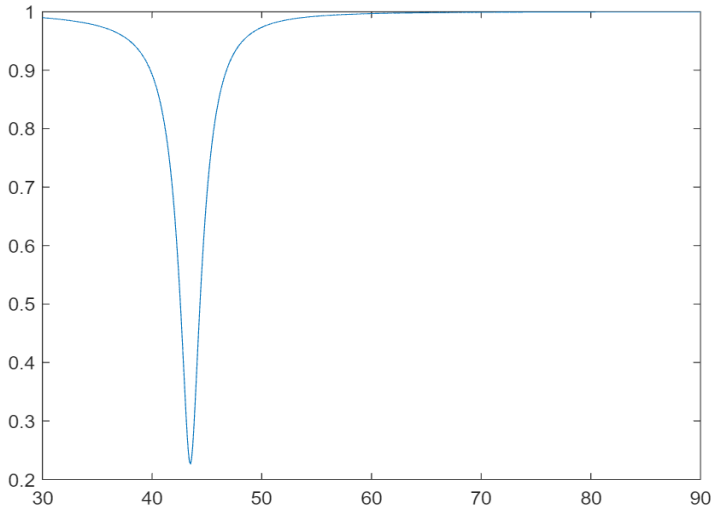

Fig. 8.1 b. From the graph where μ=1.3eV

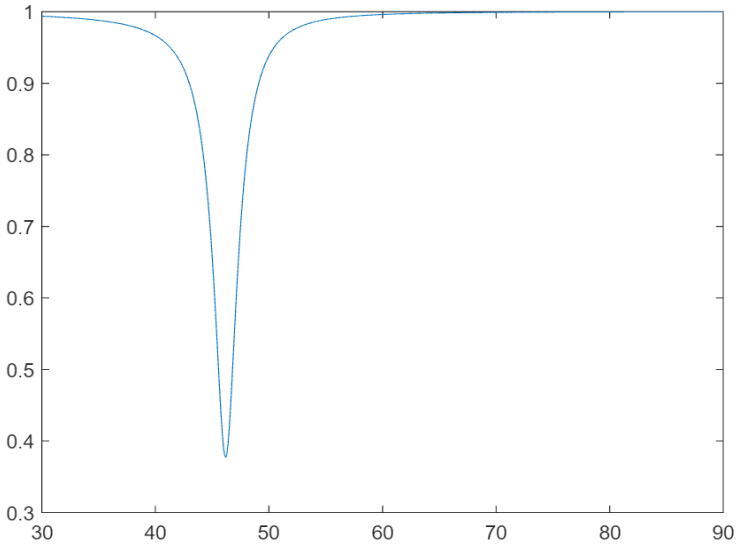

Fig. 8.1 c. From the graph where μ=1.4eV

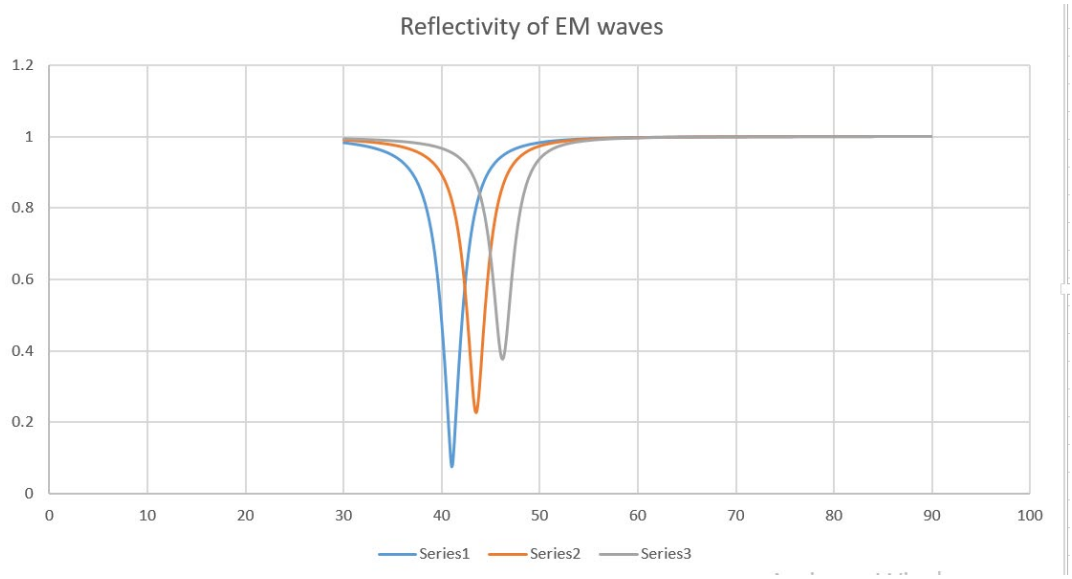

Fig. 8.1 d. From the graph where Series 1 is $\mu = 1.2eV$, Series 2 μ =1.3 eV Series 3 is $\mu = 1.4eV$

8.2 RELATIVE PHASE SHIFT WITH DIFFERENT CHEMICAL POTENTIAL

The absolute value of the reflection coefficient has a deep minimum, and giant lateral beam shifts are expected at the angles of incidence such that the beam spectrum contains the components with the same k_y as the wavenumber of the SP. It can be seen that the relative phase φ_R varies from a small negative to a large positive value when the incident angle moves through the resonant angle θ_{SP} (θ_{SP} can be derived by the phase-matching condition $k_y = k_{SP}$); thus, the large negative SGH shift can be obtained near θ_{SP}.

Again, we can obtain explicit expressions for R ($R = R_m e^{i\varphi_R}$) and T ($T = T_m e^{i\varphi_T}$) where φ_R and φ_T are the phases of the reflection and transmission coefficients, R_m and T_m represent the amplitude of the reflection and transmission coefficients respectively.

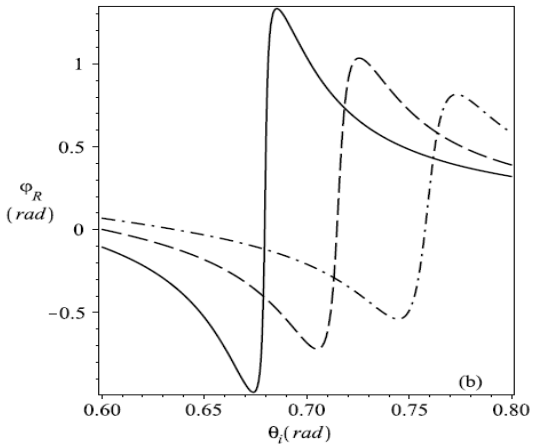

Fig. Relative phase shift waves with different chemical potential μ versus incident angle. Solid line indicates μ=1.4 eV, dashed line μ= 1. 3 eV, and dashed-dotted line μ =1.2 eV. Other parameters are ε_1 =16, ε_3= 2.5, ε_2 = 1.0, d= 3 μm, and ω =5 THz.

As we know that the gate voltage application on graphene which leads to a relation of voltage controlled Fermi energy for graphene sheet. As a consequence of tunable optical conductivity, the graphene SPP spectrum can be dynamically tuned through electrical and chemical doping.

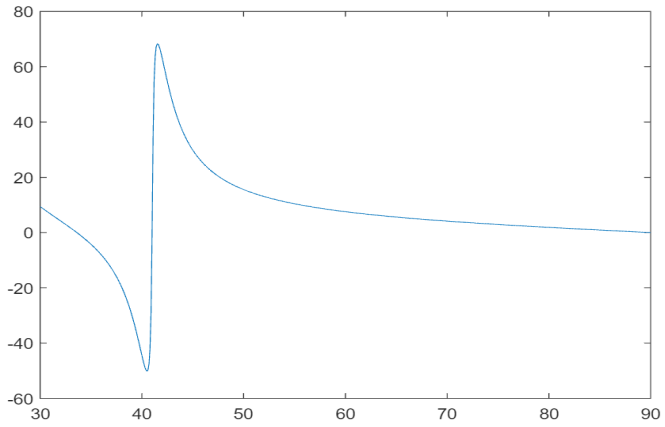

Fig. 8.2 a. From the figure where μ=1.2eV

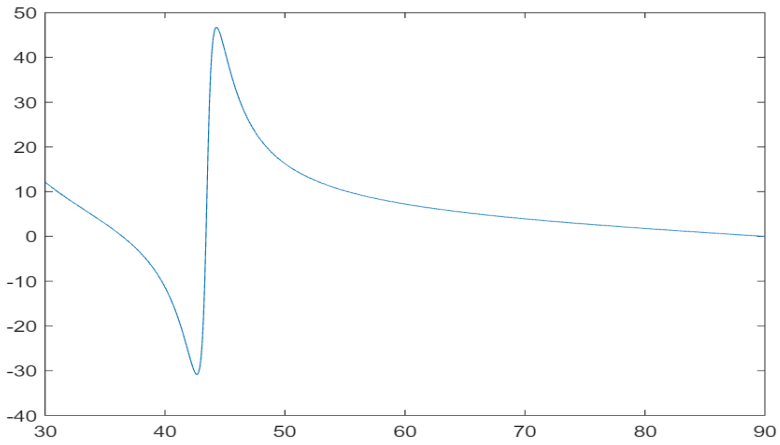

Fig. 8.2 b. From the figure where μ=1.3eV

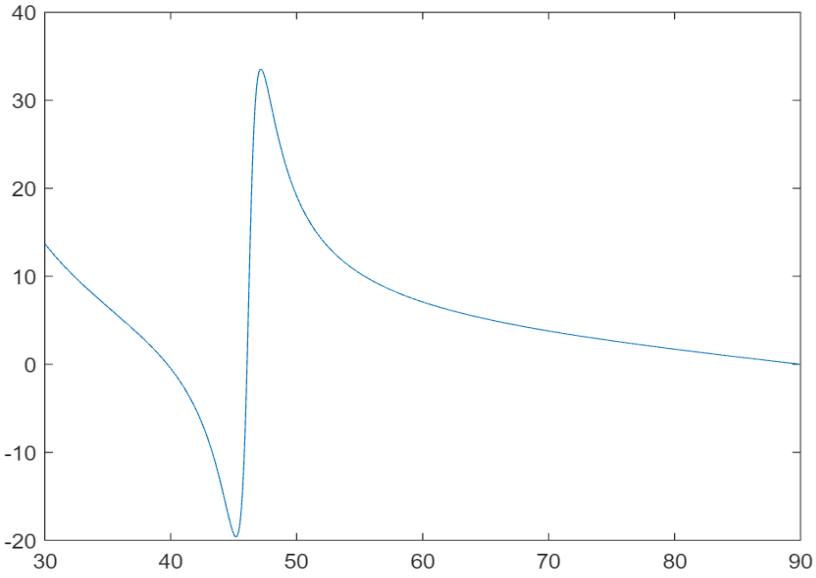

Fig. 8.2 c. From the figure where μ=1.4eV

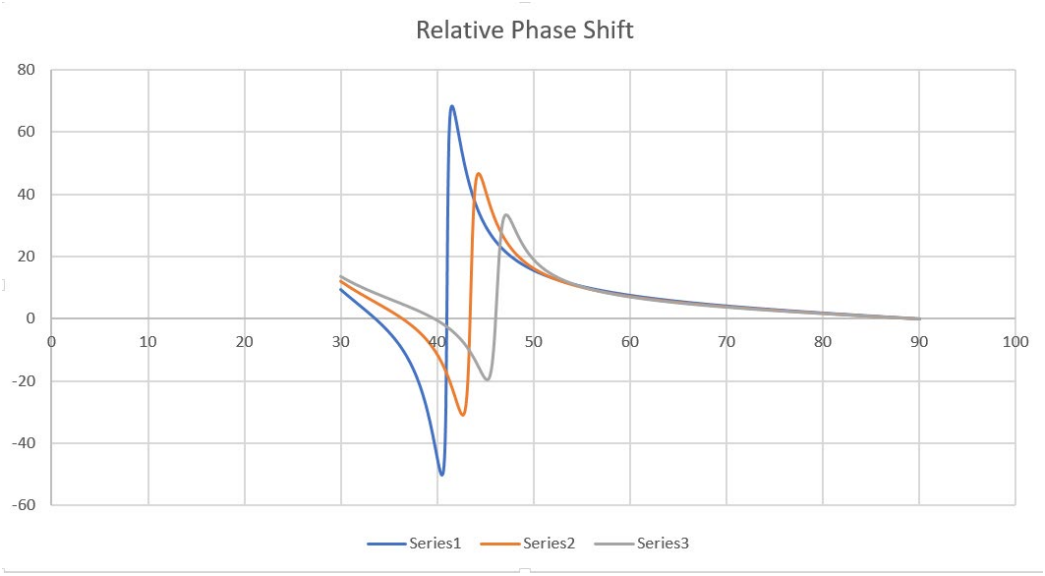

Fig. 8.2 d. From the graph where Series 1 is $\mu = 1.2eV$, Series 2 μ =1.3 eV Series 3 is $\mu = 1.4eV$

8.3 SGH SHIFTS WITH DIFFERENT CHEMICAL POTENTIAL

The direction of SGH shift may also be explained by considering an equivalent dielectric constant for graphene $\varepsilon_g = 1 + i(\sigma\eta\omega/ct)$, where $\eta \approx 377\Omega$ is the impedance of air, and $t \approx 1$ nm is the effective graphene thickness. From the equivalent dielectric constant, it is shown that $|Re(\varepsilon_g)| \gg |Im(\varepsilon_g)|$ and $Re(\varepsilon_g) < 0$. When the backward surface waves are excited, a negative shift of the beam is obtained. It is observed that the resonance dip becomes narrower and more pronounced with an increasing μ so the SGH shifts can be easily controlled by adjusting μ. The SP wavenumber decreases with increasing μ. Then the strength of the SP field that extends into region 2 decreases, and sharp narrow reflection dips occur with the reduced radiation damping of the SP mode. Then the finite slope of the relative phase change about the reflected beam becomes larger, which leads to the larger SGH shift near resonance. In contrast to the noble metal, there exists a larger wavenumber and stronger confinement of the SP mode on graphene sheets. Noble metals and left-handed metamaterials, which are

regarded as the plasmonic materials in ATR structure, are hardly tunable. Then, in the former works, once one chooses the ATR structures, it is difficult to manipulate the SGH shifts. Using the electric/magnetic field, it is a very useful way to control the chemical potential μ in order to manipulate the SGH shifts without changing or adjusting the structure of the medium.

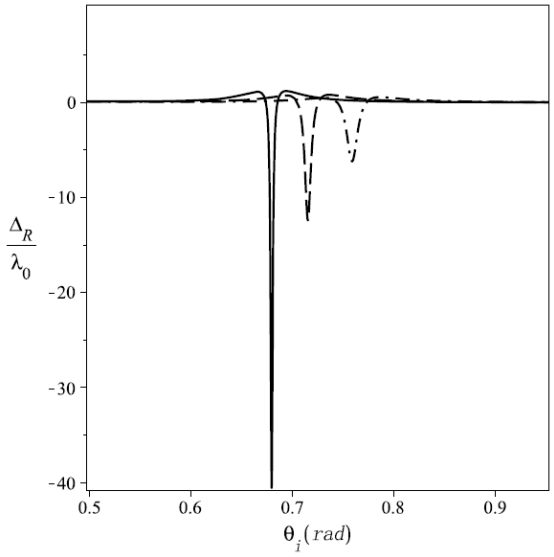

Fig. SGH shifts with different chemical potential μ versus incident angle: solid line indicates μ = 1.4 eV, dashed line μ = 1.3 eV, and dashed–dotted line μ = 1.2 eV.

As we know that the gate voltage application on graphene which leads to a relation of voltage controlled Fermi energy for graphene sheet. As a consequence of tunable optical conductivity, the graphene SPP spectrum can be dynamically tuned through electrical and chemical doping.

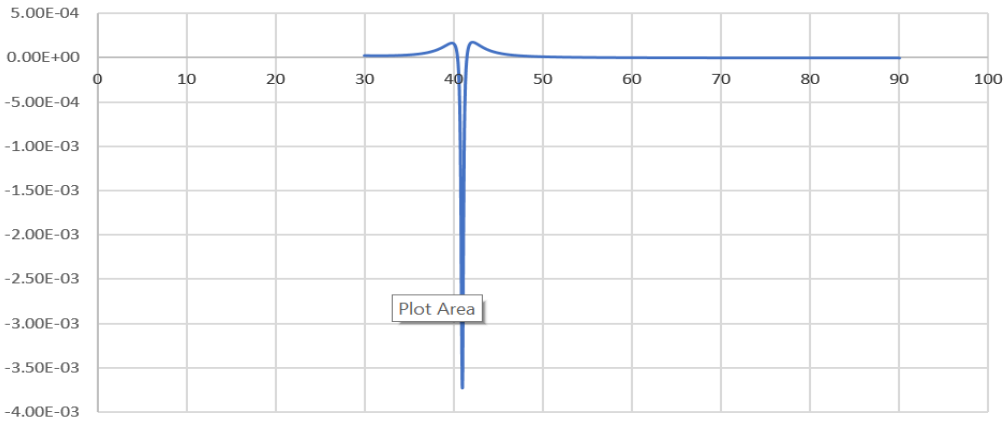

Fig. 8.3 a. From the figure where μ=1.2eV

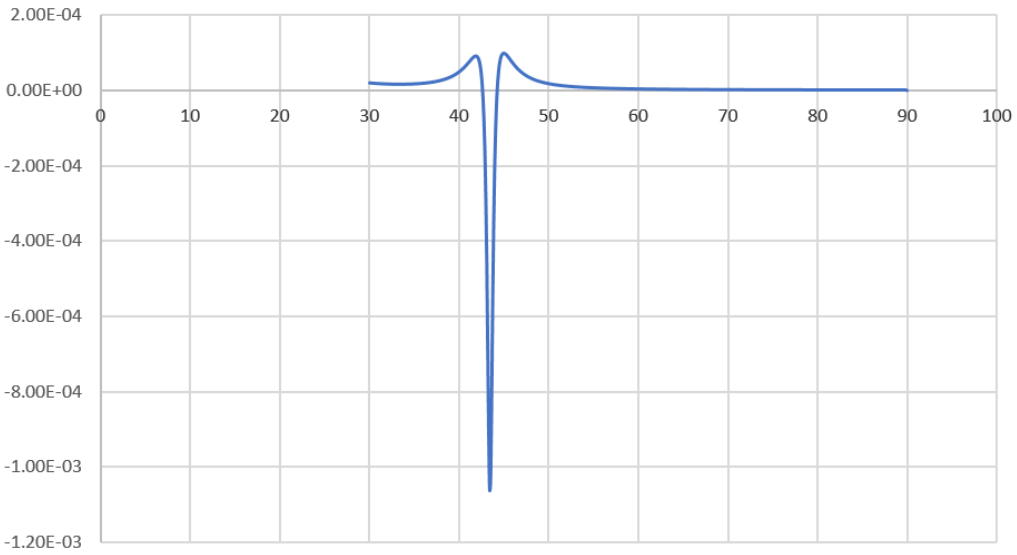

Fig. 8.3 b. From the figure where μ=1.3eV

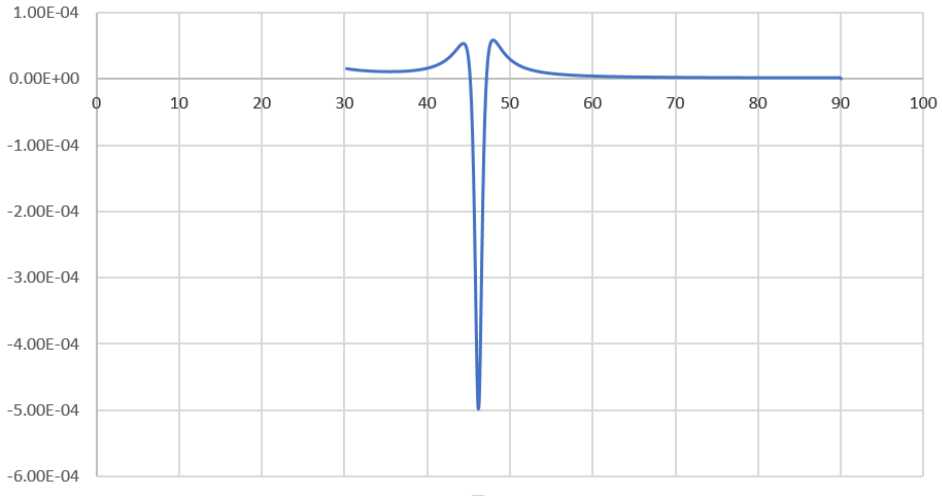

Fig. 8.3 c. From the figure where μ=1.4eV

Fig. 8.3 d. From the graph where Series 1 is $\mu = 1.2eV$, Series 2 μ =1.3 eV Series 3 is $\mu = 1.4eV$

8.4 AGH SHIFTS WITH DIFFERENT CHEMICAL POTENTIAL

We plot the AGH shift as a function of the incident angle. For a p-wave, there exists a sudden change of the sign of Θ_R near θ_{SP}, and it is observed that the AGH shift becomes larger with an increasing μ. In $|\Theta_R/\theta^2_0|$ in the Kretschmann configuration (three-layer system glass–gold–air) attains 90, which is the largest value reported ever. It is found that a great AGH effect occurs near θ_{SP}. The maximum value of $|\Theta_R/\theta^2_0|$ in this paper reaches several hundred. It is worth pointing out that, in all former investigations, the AGH shift cannot be manipulated for a fixed configuration or device. By adjusting the chemical potential μ, we can control the magnitude of the enhancement of the AGH shift. This effect provides a convenient and powerful tool for controlling the AGH shift without changing the structure, and it also provides a possibility for obtaining a large negative or positive AGH shift by changing the external electric/ magnetic field. The achievement of a giant and tunable AGH shift is quite useful for future experiments and realistic applications, such as geodetic surveying, machine-tool operation, torsion pendulum readout, atomic force microscopy, and gravitational wave detectors.

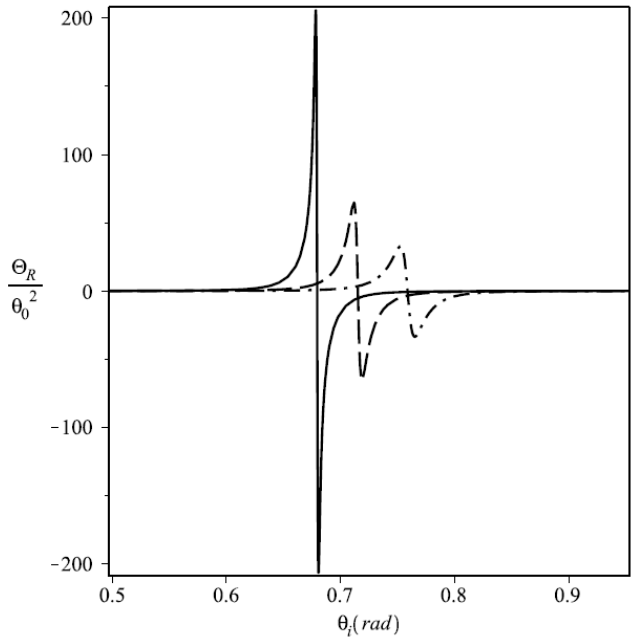

Fig. AGH shifts with different chemical potential μ versus incident angle: solid line indicates μ =1.4 eV, dashed line μ =1.3 eV, and dashed–dotted line μ =1.2 eV.

As we know that the gate voltage application on graphene which leads to a relation of voltage controlled Fermi energy for graphene sheet. As a consequence of tunable optical conductivity, the graphene SPP spectrum can be dynamically tuned through electrical and chemical doping.

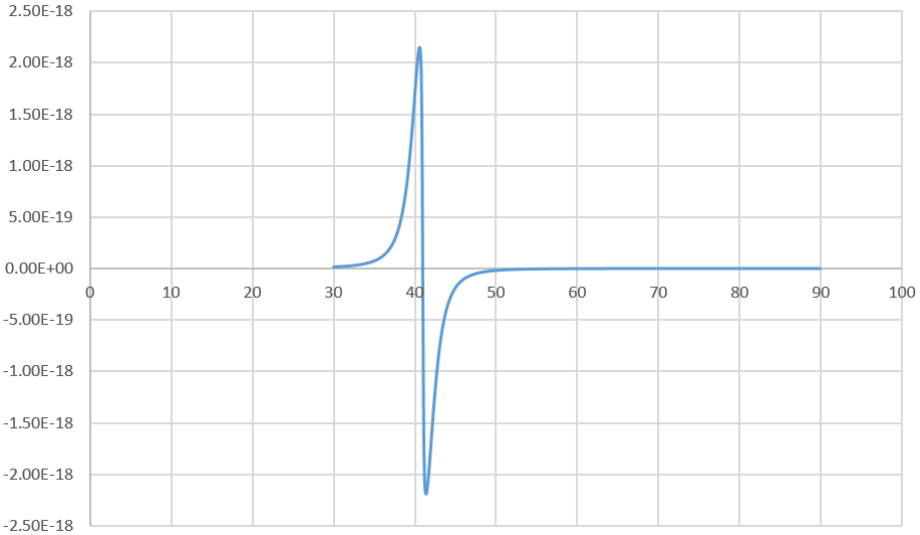

Fig. 8.4 a. From the figure where μ=1.2eV

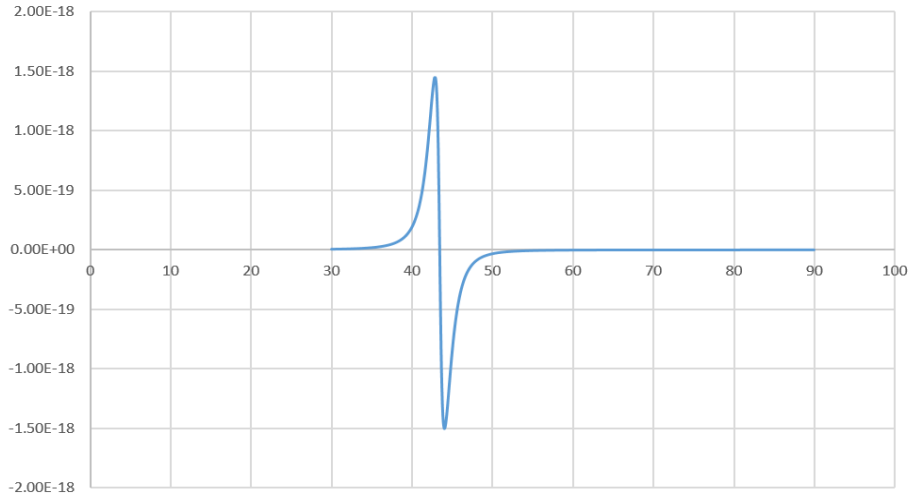

Fig. 8.4 b. From the figure where μ=1.3eV

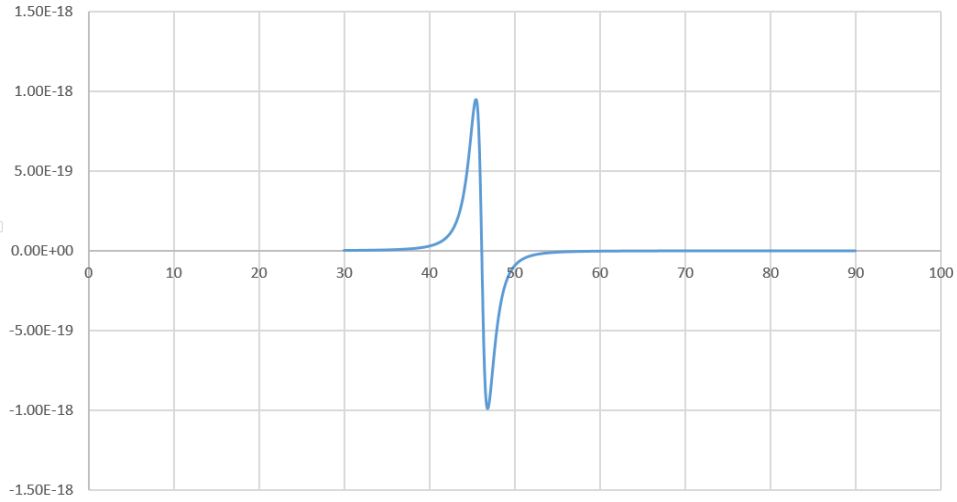

Fig. 8.4 c. From the figure where μ=1.4eV

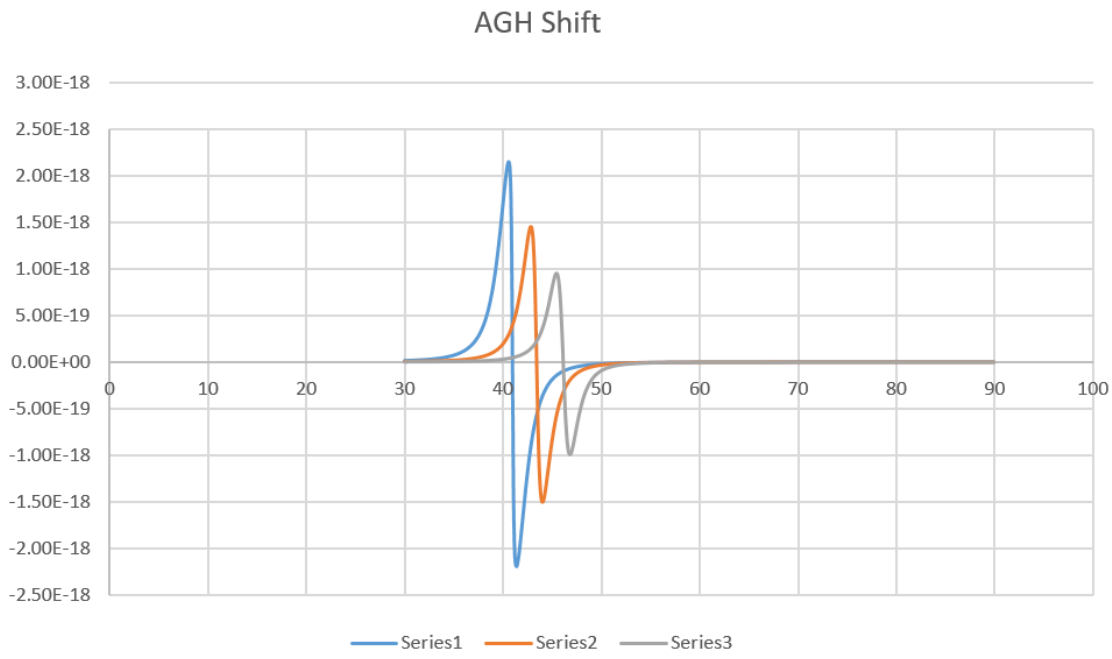

Fig. 8.4 d. From the graph where Series 1 is $\mu = 1.2eV$, Series 2 μ =1.3 eV Series 3 is $\mu = 1.4eV$

CHAPTER - 9: SUMMARY

A reflected beam could experience a lateral shift with respect to the path predicted by the geometric optics. This lateral shift is referred to as the spatial Goos–Hanchen (SGH) effect and was explained theoretically in terms of a stationary phase method. Up till now, the investigation on the SGH shift has been extended to other areas of physics, such as metamaterial, spintronics, neutron physics, and atom optics. The axis of the reflected beam could display a small angular deviation from the law of specular reflection. This effect is referred to as the angular Goos–Hanchen (AGH) shift and has been the subject of a number of theoretical investigations. Recently, the experimental proofs of the AGH shift have been reported. In the case of a single dielectric interface, the SGH shift is of the order of the wavelength. It has been reported that giant SGH shifts may occur in the layered systems supporting surface plasmons (SPs), which are able to transfer energy along the incident interface. Excitations of SPs take place in two well-known attenuated total reflection (ATR) structures: the so-called Otto configuration and Kretchmann configuration. Enhancement of the AGH shift can be found in the Kretschmann configuration.

Recently, it has been reported that bistable SGH shifts can be found in an ATR structure with Kerr-type nonlinearity, which can be used to control the SGH shifts. In the former ATR structures, plasmonic materials are noble metal or left-handed metamaterial, which is hardly tunable and exhibits large losses. More recently, it has been found that SP modes can also be supported in graphene, a single layer of carbon atoms gathered in a honeycomb lattice, at infrared and terahertz frequencies. By applying a gate voltage, the transport properties of graphene can be readily modulated and can be applied to various plasmonic devices the beam reflection from an ATR structure containing a graphene layer and calculate these SGH and AGH shifts as functions of the incidence angle showing that they are strongly enhanced in correspondence with the SP resonant angle. Here, by using graphene we propose an alternative method of controlling the GH shifts, which leads to the superior sensitivity of the SP sensor.

CHAPTER - 10: DISCUSSION

Recently, the experimental proofs of the AGH shift have been reported. In the case of a single dielectric interface, the SGH shift is of the order of the wavelength. It has been reported that giant SGH shifts may occur in the layered systems supporting surface plasmons (SPs), which are able to transfer energy along the incident interface.

We will try to manipulate and change the various data to figure out more about its AGH and SGH characteristics. We will also try to increase this lateral SGH and Angular AGH shifts to a greater extent in future with reference to the project.

CHAPTER - 11: CONCLUSION

The relative phase φ_R varies from a small negative to large positive value when the incident angle moves through the resonant angle θ_{SP} (θ_{SP} can be derived by the phase matching condition $k_y = k_{SP}$). Thus, the large negative SGH shift can be obtained near θ_{SP}. It is observed that the resonance dip becomes narrower and more pronounced with an increasing μ so the SGH shifts can be easily controlled by adjusting μ.The SP wavenumber decreases with increasing μ. Then the strength of the SP field that extends into region 2 decreases, and sharp narrow reflection dips occur with the reduced radiation damping of the SP mode. Then the finite slope of the relative phase change about the reflected beam becomes larger, which leads to the larger SGH shift near resonance. A dc gate is applied on the graphene sample, the ac modulation can be added to the dc gate voltage, which changes the charge carrier density in graphene. Then the value of chemical potential μ can be tuned by an electric/magnetic field. By using the electric/magnetic field, it is a very useful way to control the chemical potential μ in order to manipulate the SGH shifts without changing or adjusting the structure of the medium properties, recently graphene photonics have been stretched to nonlinear optical bistable devices.

In conclusion, the giant GH shifts can be observed from an Otto structure containing a graphene layer when the SP resonance is properly excited. By modulating the voltage applied to graphene via an external gate, the GH shifts can be controlled. The superior sensitivity of the SP sensor can be obtained by using an alternative SP sensing scheme based on the giant and tunable GH shifts. As an alternative, if the graphene sample can be directly deposited onto region 2 in the Kretschmann configuration may be employed. It should be noted that the separation of the spatial and angular GH shifts is artificial. In a unified description for the spatial and angular GH shifts that reveals the duality between spatial and angular shift is reported. According to the expression of k_{SP}, a different frequency for the incident wave can change the SP resonance conditions and affects the GH shifts. It must be pointed out that, to stay within the regime for which our analysis is valid, the frequency for the incident wave is limited near the THz regime. In other frequency ranges, considering the effects of some physical factors, such as the effects of free-carrier absorption, the setting about conductivity and the relaxation time will be amended.

CHAPTER - 12: BIBLIOGRAPHY

i. Journals

F. Goos and H. Hachen, “Ein neuer und fundamentaler versuch zur total reflektion,” Ann. Phys. 1, 333–346 (1947).

K. V. Artmann, “Berechnung der Seitenversetzung des total reflektierten strahles,” Ann. Phys. 1, 87–102 (1948).

H. K. V. Lotsch, “Beam displacement at total reflection: the Goos–Hänchen effect,” Optik 32, 116–137 (1970).

X. Chen, C.-F. Li, and Y. Ban, “Tunable lateral displacement and spin beam splitter for ballistic electrons in two-dimensional magnetic-electric nanostructures,” Phys. Rev. B 77, 0733071 (2008).

X. Chen, X.-J. Lu, Y. Wang, and C.-F. Li, “Controllable Goos–Hänchen shifts and spin beam splitter for ballistic electrons in a parabolic quantum well under a uniform magnetic field,”Phys. Rev. B 83, 1954091 (2011).

C. C. Chan and T. Tamir, “Angular shift of a Gaussian beam reflected near the Brewster angle,” Opt. Lett. 10, 378 380 (1985).

ii. Books/Articles

“Journal of the Optical Society of America B” by OSA Publishing

iii. Sites

https://en.wikipedia.org/wiki/Surface_plasmon

https://en.wikipedia.org/wiki/Surface_plasmon_resonance

https://en.wikipedia.org/wiki/Graphene

https://en.wikipedia.org/wiki/Total_internal_reflection

https://www.osapublishing.org/josab/abstract.cfm?URI=josab-31-10-2325